



Working backwards from streambed thermal anomalies: hydrogeologic controls on preferential brook trout spawning habitat in a coastal stream

Martin A. Briggs^{1*}, mbriggs@usgs.gov, (phone) +1.860.487.7402

Judson W. Harvey²

Stephen T. Hurley³

Donald O. Rosenberry⁴

Timothy McCobb⁵

Dale Werkema⁶

John W. Lane, Jr.¹

¹U.S. Geological Survey, Hydrogeophysics Branch, 11 Sherman Place, Unit 5015, Storrs, CT, 06269 USA

²U.S. Geological Survey, National Research Program, Reston, VA, 20192 USA

³Massachusetts Division of Fisheries and Wildlife, 195 Bournedale Road, Buzzards Bay, MA, 02532 USA

⁴U.S. Geological Survey, National Research Program, M.S. 406, Bldg. 25, DFC, Lakewood, CO, 80225 USA

⁵U.S. Geological Survey, 10 Bearfoot Road, Northborough, MA, 01532 USA

⁶U.S. Environmental Protection Agency, Office of Research and Development, National Exposure Research Laboratory, Exposure Methods & Measurement Division, Environmental Chemistry Branch, Las Vegas, NV, 89119 USA



35 **Abstract:**

36 Brook trout (*Salvelinus fontinalis*) spawn in fall, and overwintering egg development
37 can benefit from stable, relatively warm temperatures in groundwater seepage zones. However,
38 eggs also are sensitive to dissolved oxygen concentration, which may be reduced in discharging
39 groundwater. We investigated a 2-km reach of the coastal Quashnet River, Cape Cod,
40 Massachusetts, USA, to relate preferred fish spawning habitat to geology, geomorphology, and
41 groundwater discharge. Thermal reconnaissance methods were used to locate zones of rapid
42 groundwater discharge, which were predominantly found along the center channel of a wider
43 stream valley section. Pore-water chemistry and temporal vertical groundwater flux were
44 measured at a subset of these zones during field campaigns over several seasons. Seepage zones
45 in open valley sub-reaches generally showed suboxic conditions and higher dissolved solutes
46 compared to the underlying glacial outwash aquifer. These discharge zones were cross-
47 referenced with preferred brook trout redds, evaluated during 10 yr of observation, all of which
48 were associated with discrete alcove features in steep cut banks where stream meander bends
49 intersect the glacial valley walls. Seepage in these repeat spawning zones was generally stronger
50 and more variable than open valley sites, with higher dissolved oxygen and reduced solute
51 concentrations. The combined evidence indicates that regional groundwater discharge along the
52 broader valley bottom is predominantly suboxic due to the influence of near-stream organic
53 deposits; trout show no obvious preference for these zones when spawning. However, the
54 meander bends that cut into sandy deposits near the valley walls generate strong, oxic seepage
55 zones that are utilized routinely for redd construction and the overwintering of trout eggs. In
56 similar coastal systems with extensive valley peat deposits, specific use of groundwater
57 discharge points by brook trout may be limited to morphologies such as cut banks where
58 groundwater flowpaths can short circuit buried organic material and remain oxygen rich.



59 Introduction

60 The heat tracing of waters can be used to map a distribution of discrete groundwater
61 discharge zones throughout surface water systems at times of contrast between surface and
62 groundwater temperature. The measurement of water temperature from the reach to watershed
63 scale is now possible using thermal infrared (TIR) and fiber-optic distributed temperature
64 sensing (FO-DTS) methodology (Hare et al., 2015). Remote TIR data collection throughout the
65 river corridor has been enabled by handheld cameras, piloted aircraft, and the rapidly evolving
66 capabilities of Unmanned Aircraft Systems. Researchers are capitalizing on the ongoing
67 refinement of these technologies to identify zones of focused groundwater seepage to streams to
68 map potential discrete preferential cold-water fish habitat such as summer thermal refugia
69 (Dugdale et al., 2015). However, surface thermal surveys alone do not indicate groundwater
70 flowpath dynamics or the suitability of interface aquatic habitat.

71 For example, dissolved oxygen (DO) concentration must be sufficiently high for cold
72 groundwater seepage to provide support for fish life-processes at the direct point of discharge to
73 surface water (Ebersole et al., 2003), which is not apparent from thermal analysis alone. During
74 summer warm periods in systems with suboxic groundwater, managed cold-water fish species
75 such as salmonids can face a tradeoff between occupying discrete zones of preferred water
76 temperatures with near-lethal DO levels, or stream sections that are too warm for long-term
77 survival (Mathews and Berg, 1997). The use of groundwater upwelling zones as thermal refugia
78 is further complicated by competition with aggressive invasive species (to the Northeastern
79 USA) such as brown trout that compete with native trout for resources (Hitt et al., 2017).
80 Streams at higher elevations may support reach-scale cold water habitat where point-scale
81 thermal refugia are not needed under current climatic conditions, serving as vital “climate



82 refugia” against rising air temperatures (Isaak et al., 2015). In systems with reliably cold channel
83 water in summer, which can also exist at low elevations when heavily influenced by discharging
84 groundwater, salmonid fish may directly use groundwater seepage zones for spawning rather
85 than thermal refuge.

86 Brook trout (*Salvelinus fontinalis*) are a species of char that are native to eastern North
87 America, from Georgia to Quebec (MacCrimmon and Campbell, 1969). Populations have been
88 stressed by warming temperatures and reduced water quality, particularly in low-elevation areas
89 (Hudy et al., 2008). Stream network-scale tracking of fish has indicated brook trout directly
90 utilize stream confluence mixing zones and groundwater upwelling to survive warm summer
91 periods (Baird and Krueger, 2003; Petty et al., 2012; Snook et al., 2016). Additionally, brook
92 trout spawn in the fall, and eggs deposited in redds therefore develop over the winter before
93 hatching in spring (Cunjak and Power, 1986). Oxygen use by the shallow buried embryos
94 increases over the period of development (Crisp, 1981), and therefore DO concentration is a
95 critical parameter of the pore waters in which the eggs are bathed. Several studies have
96 demonstrated the importance of hyporheic downwelling in increasing shallow oxygen
97 concentrations specifically at salmonid redds when streambed pore water is generally reduced in
98 DO (e.g. Buffington and Tonina 2009; Cardenas *et al.* 2016). Fine sediments can reduce the
99 efficacy of hyporheic DO exchange in spawn zones (Obruca and Hauer, 2016), and are actively
100 cleared by trout during the spawning process ((Montgomery et al., 1996).

101 The importance of hyporheic exchange to salmonid spawning may be limited in the
102 lowland streams that are expected to harbor native cold-water species in the 21st century: those
103 with strong groundwater influence. Groundwater upwelling reduces the penetration of hyporheic
104 flow from surface water (Cardenas and Wilson, 2006) and may shut down hyporheic flushing in



redds (Cardenas et al., 2016). Where hyporheic exchange does introduce oxygenated channel water into the shallow streambed, the downward advection of heat associated with near-freezing surface water in winter will also cool streambed sediments (Geist et al., 2002), potentially impairing egg development. Coaster brook trout, a life-history variant of native brook trout exhibiting potadromous migrations within the Great Lakes, have been shown to specifically prefer groundwater discharge zones for building redds (Grinsven et al., 2012). The development of trout in winter has been found to be positively correlated with warmer stream water temperatures as influenced by groundwater seepage (French et al., 2016), and therefore spatially discrete groundwater discharge zones with adequate DO may form preferred brook trout spawning habitat (Curry et al., 1995).

Multiscale physical and biogeochemical factors influence temperature and DO concentrations along groundwater flowpaths. In river valleys, discharge to surface water of locally recharged groundwater is expected to emanate from more shallow, lateral flowpaths controlled by local topography (Modica, 1999; Winter et al., 1998). Deeper regional discharge is expected to be more vertical through the streambed, as shown using our study site-specific topography in conceptual Figure 1a. Shallow groundwater flowpaths, particularly those within approximately 5 m of the land surface, will be more sensitive to annual air temperature patterns and longer term warming trends due to strong vertical conductive heat exchanges (Kurylyk et al., 2015). The distance of seeps from upgradient groundwater recharge zones will also affect seepage temperature dynamics and associated aquatic ecosystems due to future changes in temperature or precipitation (Burns et al., 2017). Therefore, working backwards from thermal anomalies into the landscape is critical to understanding the thermal stability of current and future point-scale preferential brook trout habitat (Briggs et al., 2017a). The complimentary



128 methodology of geophysical remote sensing, geochemical sampling, and vertical bed
129 temperature time series can indicate the physical and chemical properties of groundwater
130 flowpaths that source seepage zones utilized routinely by fish.

131 Coarse-grained mineral-dominated aquifers with little fine particulate organic matter and
132 low dissolved organic carbon supply tend to result in generally oxic groundwater conditions
133 (Back et al., 1993). The sandy surficial aquifer of Cape Cod, where our investigation took place,
134 is a good example of a mineral soil-dominated flow system (Frimpter and Gay, 1979). Flow of
135 groundwater through near-stream organic deposits, however, can result in inverted redox
136 gradients toward the upwelling interface, such that groundwater discharged to surface water is
137 reduced in DO (Seitzinger et al., 2006). In sandy glacial terrain with superimposed peatland
138 deposits, the specific flow patterns of groundwater to surface water in relation to buried peat will
139 influence groundwater discharge biogeochemistry. Krause *et al.* (2013) found that streambed
140 groundwater seepage was reduced in DO in zones with peat deposits, likely due to an increase in
141 both near-stream residence time and localized source of dissolved organic carbon. Whether or
142 not groundwater flowpaths are dominated by local or regional topography will influence where
143 and how groundwater discharges to surface water, including possible contact with near-stream
144 organic deposits (Figure 1a).

145 Interdisciplinary collaborations between physical and biological scientists are useful to
146 better understand how cold-water species utilize groundwater seepage-influenced stream habitat,
147 and the larger landscape-scale controls on seepage zone characteristics. While previous
148 hydrogeological research in the coastal stream used for this study had focused on locating and
149 quantifying discrete groundwater discharge (e.g. “cold anomalies”, Hare et al., 2015; Rosenberry
150 et al., 2016), here we endeavor to understand the hydraulic and biogeochemical controls on



151 seepage zone distribution utilized directly by native brook trout. In this groundwater-dominated
152 stream (e.g. likely climate refugia), brook trout do not need to occupy discrete inflows for
153 summer thermal refugia, but do favor certain upwelling zones for fall spawning. We compare
154 over a decade of visual and electronic-tag data regarding brook trout redds to a comprehensive
155 physical and chemical characterization of groundwater seepage zones to:

- 156 1. Identify preferred brook trout spawning locations, determine if they are directly
157 associated with groundwater upwelling, and identify common characteristics (e.g.
158 temperature, dissolved constituents) between these zones.
- 159 2. Develop a hydrogeological understanding of trout-preferred groundwater discharge
160 zones that can aid in their identification in other less-studied systems.

161 **Site Description and Previous Ecologic and Hydrogeologic Characterization**

162 Cape Cod is a peninsula in southeastern coastal Massachusetts, USA, composed
163 primarily of highly permeable unconsolidated glacial moraine and outwash deposits. The largest
164 of the Cape Cod sole-source aquifers occupies a western (landward) section of the peninsula
165 (LeBlanc et al., 1986), and is incised by several linear valleys that drain groundwater south to the
166 Atlantic Ocean via baseflow-dominated streams (Figure 2a). Strong groundwater discharge to
167 one such stream, the Quashnet River, supports a relatively stable flow regime that has averaged
168 0.49 ± 0.15 (SD) $\text{m}^3 \text{s}^{-1}$ from 1986-2015 (Rosenberry et al., 2016). The lower Quashnet River
169 emerges from a narrow sand and gravel valley to a broader area with well-defined lateral
170 floodplains. Historical cranberry farming practices, abandoned in the 1950s, have modified the
171 stream corridor (Barlow and Hess, 1993). Primary modifications included straightening of the
172 main channel (reducing natural sinuosity), installation of flood-control structures, incision of



173 shallow groundwater drainage ditches in the lateral peatland floodplain, and widespread
174 application of sand to the floodplain surface. The current bank-full width of the main channel
175 averages approximately 4 m.

176 The Quashnet River has long been recognized as critical habitat for a naturally reproducing
177 population of native sea-run brook trout (Mullan, 1958) with a genetically distinct population
178 (Annett et al., 2012). Efforts to restore trout habitat by the group *Trout Unlimited* and others
179 have been ongoing for over 40 yr (Barlow and Hess, 1993). These efforts include the removal of
180 flood-control structures and planting of trees along the main channel, and addition of wood
181 structures to stabilize banks and provide cover from airborne predators. Further, the
182 Commonwealth of Massachusetts purchased 31 acres in 1956 and an additional 360 acres along
183 the lower Quashnet River in 1987 and 1988 to protect the area from development. The
184 Massachusetts Division of Fisheries and Wildlife has been monitoring trout populations since
185 1988 and movement since 2007.

186 Groundwater influence on stream temperature is pronounced, particularly over the 2-km
187 reach above the USGS gage, below which stream stage is tidally affected. Temperature
188 influences in summer include a general downstream cooling with distance toward the USGS
189 gage (Hare et al., 2015; Rosenberry et al., 2016). Ambient regional groundwater temperature is
190 approximately 11 °C (Briggs et al., 2014), and strong conductive and advective exchange with
191 the proximal aquifer maintains surface water temperature well below the lethal threshold for
192 brook trout (maximum weekly average temperature >23.3 °C, Wehrly *et al.* 2007). Therefore
193 niche-scale thermal refugia are not a current concern in this system, as the stream supports
194 system-scale cold-water habitat that is likely to persist into the future. In winter, seepage zones
195 can be located as relatively warm anomalies (Hare et al., 2015) increasing and buffering surface



196 water temperatures from ambient atmospheric influence.

197 Previous work has measured relatively large net gains in streamflow over the lower Quashnet
198 River (Barlow and Hess, 1993; Rosenberry et al., 2016), attributed to groundwater discharge
199 through direct streambed seepage and harvesting of groundwater from the floodplain platform
200 via relic agricultural drainage ditches. Repeat deployments of fiber-optic temperature sensing
201 (FO-DTS) cables along the thalweg streambed interface (June 2013, 2014) indicate the greatest
202 density of focused seepage zones occurs along the broader valley area approximately 1 km
203 upstream of the USGS gage; this zone coincides with the largest gains in net streamflow (Hare et
204 al., 2015). Based on the streambed interface temperature data presented by Rosenberry et al.
205 (2016), Figure 1b shows how temperature-sensitive fiber optic cables have been used to pinpoint
206 possible groundwater discharge zones based on anomalously cold mean temperature and/or
207 reduced thermal variance. Focused evaluation of FO-DTS anomalies with physical seepage
208 meters and vertical temperature profilers confirmed localized, meter-scale seepage zonation
209 along the streambed (Briggs et al., 2014; Irvine et al., 2016a), where discrete colder zones
210 indicated through heat tracing showed approximately 5 times the groundwater discharge rate of
211 adjacent sandy bed locations only meters away (Rosenberry et al., 2016). Active heating of
212 wrapped FO-DTS cables deployed vertically within an open valley streambed seepage zone
213 indicated true vertical flow to at least 0.6 m into the bed sediments (Briggs et al., 2016b), an
214 expected characteristic of more regional groundwater discharge (Winter *et al.* 1998; Figure 1a),
215 rather than that driven by topography local to the river. Hyporheic exchange in the lower
216 Quashnet River system is superimposed on the general upward hydraulic gradient to the stream,
217 and therefore reduced to a thin, shallow hyporheic exchange zone (e.g. < 0.1 m depth) along the
218 thalweg by these competing pressures (Briggs et al., 2014; Rosenberry et al., 2016), as has been



219 shown for similar systems (e.g. Cardenas and Wilson 2006).

220 **Methods**

221 A combination of fish tagging, geophysical surveys, and focused pore-water sampling
 222 was used to investigate the interplay between the locations of preferential brook trout spawning
 223 and the local hydrogeology. For consistency, we adopt the numerical naming convention of
 224 (Rosenberry et al., 2016) for previously identified persistent streambed seepage zones as shown
 225 in Figure 1b. We also refer to the 3 sites of known repeated trout spawning activity as Spawn 1,
 226 2, and 3, from upstream to downstream, respectively (Figure 2).

227 *Brook trout spatial behavior*

228 Observations regarding brook trout spawning locations were made as part of an ongoing
 229 PIT (Passive Integrated Transponder) tagging study of the native reproducing population of the
 230 Quashnet River. Large-scale trout movements are continuously monitored in the lower Quashnet
 231 River at 3 stationary fish counting sites (Figure 2a). However the spatial resolution of these
 232 counting sites, separated by hundreds of meters, is not adequate to study how brook trout utilize
 233 specific decimeter- to meter-scale groundwater discharge zones. For this finer scale
 234 characterization, fish tags have also been located through roving surveys using a handheld
 235 portable PIT antenna (Biomark, Inc.) conducted in spring and fall since 2007. In addition to
 236 tagged fish location at the time of these surveys, spawning brook trout were located visually
 237 during fall data collection events and clustering behavior captured within one seepage feature by
 238 underwater video in 2015 using a GoPro Hero camera (San Mateo, CA). Also the dropout of PIT
 239 tags from the fish body is a process that is more likely to happen during spawning behavior in
 240 salmonids (Meyer et al 2011), so dropped tags were located and spatially mapped.

241 *Fiber-optic distributed temperature sensing*

242 To augment previously existing streambed interface thermal surveys for groundwater
243 discharge (e.g. Rosenberry et al., 2016; Figure 1b), ruggedized fiber-optic cables suitable for
244 stream use were deployed along each bank from approximately 160 m upstream of the middle
245 fish counter through the Spawn 3 meander bend for approximately 450 m total length (Figure
246 2a). Two separate cables weighted with stainless steel armoring were installed directly along the
247 foot of each bank on top of the streambed interface. Single-ended measurements made at the
248 1.01 m linear spatial sampling scale were integrated over 5-min intervals on each channel by an
249 Oryx FO-DTS control unit (Sensornet Ltd.). During the same period, data were also collected
250 along a high-resolution wrapped fiber-optic array for a dataset described in Kurylyk *et al.* (2017)
251 but not shown here; this experimental setup resulted in measurements for each channel of 4
252 instrument channels recorded at 20-min intervals. Calibration for dynamic instrument drift was
253 performed automatically using an approximately 30-m length of cable for each channel
254 submerged in a continuously mixed ice-bath and monitored with an independent Oryx T-100
255 thermistor.

256 *Ground Penetrating Radar*

257 Ground penetrating radar (GPR) has been successfully applied to several surface
258 water/groundwater exchange studies to characterize underlying peat and sandy deposits (e.g.
259 Lowry *et al.* 2009; Comas *et al.* 2011) due to strong expected differences in matrix porosity
260 (water content), which can exceed 70% in peat (Rezanezhad et al., 2016). An upstream to
261 downstream GPR profile was collected on July 7, 2016 using a MALA HDR GX160 shielded
262 antenna (MALA GPR, Sweden) hand-towed down the thalweg from a small inflatable
263 watercraft. The locations of major seep and spawning sites were marked on the digital GPR



record during data collection. The GPR data were processed using Reflexw software (Sandmeier, Germany) to convert reflection time to interface depth.

Temporal groundwater discharge characterization

Temporal patterns in vertical groundwater discharge flux rate can indicate source flowpath hydrodynamics, and can be derived from bed temperature time series, as reviewed by Rau et al., (2013). Custom “1DTempProfilers” designed specifically for the quantification of groundwater upwelling (Briggs et al., 2014) were used to monitor streambed temperature over time along a shallow vertical profile. Profilors were deployed in zones of known focused groundwater discharge and/or preferential trout spawning from June 11 (day 162) to July 13 (day 193) in 2014; August 21 (day 233) to September 13 (day 247) in 2015; and June 5 (day 157) to July 9 (day 191) in 2016. Individual thermal data loggers (iButton Thermochron DS1922L, Maxim Integrated) were waterproofed with silicone caulking and inserted horizontally into short slotted-steel pipes (0.025 m diameter). The shallow thermal profilors were driven vertically into the streambed so that sensors were positioned at some combination of 0.01, 0.04, 0.07, and 0.11 m depths. Data were collected at temporal intervals of 0.5 hr in 2014, 2015, and 1 hr in 2016. Rosenberry *et al.* (2016a) found that when a subset of the 2014 streambed temperature data presented here were analyzed using the diurnal signal amplitude attenuation models employed by VFLUX2 (Irvine et al., 2015), a near 1:1 relation was found in comparison to physical seepage meter measurements of groundwater discharge ranging from 0.5 to 3 m d^{-1} . This strong relation was likely enabled by using in-situ measurements of thermal diffusivity (K_e) for modeling as suggested by Irvine *et al.* (2016) using the diurnal signal phase and amplitude relations presented by Luce *et al.* (2013). A sequential diurnal signal-based K_e evaluation to inform amplitude attenuation-based analytical fluid flux modelling was used here, and this approach is described in



287 detail by Irvine et al., (2016b).

288 *Geochemical pore-water characterization*

289 Subsurface water samples were collected for chemical analysis at ten locations in the
290 stream along the 2-km study reach using 0.0095 m (nominal) stainless steel drivepoints that had
291 been inserted to depths of 0.3, 0.6, and 0.9 m. A 2.4-m length of relatively gas-impermeable
292 tubing (Masterflex norprene size 15) was attached to the drivepoint and a peristaltic pump was
293 used to pump groundwater samples until free of obvious turbidity (typically requiring 3 min of
294 pumping) after which the pumping rate was slowed and, the groundwater samples were collected
295 by pumping into 60-mL HDPE syringe barrels. First an unfiltered sample for specific
296 conductivity was pushed from the syringe into a 30-mL HDPE Nalgene sample bottle. Second, a
297 filtered sample for anion analysis was collected after attaching a 0.2- μ m pore size (25-mm
298 diameter) Pall polyethersulfone filter to the syringe. Lastly, the pumping rate was slowed again
299 and an overflow cup was attached to the norprene sample tubing and held upright until
300 overflowing, at which point DO was measured by a field colorimetric test using the
301 manufacturer's evacuated reagent vials, which were snapped inside the overflow cup and then
302 read on the field photometer (Chemetrics V-2000). DO concentrations were read twice and the
303 test repeated using an alternative vial kit if results were near the concentration range limit or out
304 of range. The collected samples were kept cool and out of the light and analyzed for Cl^- upon
305 return to the laboratory using standard ion chromatographic techniques.

306 Pore-water samples also were collected from shallow depths ranging between 0.015 and
307 0.15 m below the streambed surface at the same locations as the drivepoints using minipoint
308 samplers (e.g. Harvey and Fuller 1998). These small-volume water samples were collected at
309 slow rates using 0.32-cm stainless steel tubes with slots of 0.01 m forming the screen 0.005 m



310 behind a clamped tip. The sample tubes were pre-aligned for deployment at selected depths
311 (0.015, 0.04, 0.08 and 0.15 m) by passing each tube through fittings that gripped the tubes in an
312 acrylic disc that was lowered until the slotted ends of the sample tubes reached the desired
313 depths. Water was pumped simultaneously from all depths using a multi-head pump that
314 withdrew small-volume samples (15 mL) at low flow rates (1.5 mL min^{-1}) to minimize
315 disturbance of natural subsurface fluxes and chemical gradients. Pumped lines terminated at
316 press-on luer fittings that were pushed onto 0.2- μm pore size (25-mm diameter) Pall
317 polyethersulfone filters. Samples for specific conductivity were collected whereas filtered
318 samples were collected for anions in prelabeled 20-mL LDPE plastic scintillation vials with
319 PolysealTM caps. Sample lines were then attached to overflow cups and dissolved oxygen
320 concentrations were measured as described above.

321 As mentioned previously, historic cranberry farming practices modified the Quashnet
322 River valley including the incision of drainage ditches into the floodplain. Some ditches extend
323 from the valley wall to the main channel, whereas others are shorter or cut at angles. In addition
324 to characterization of pore water, 34 major drainage ditches (observed flowing water) and a
325 stream thalweg profile were spot checked for specific conductivity on June, 16 2014 (day 167)
326 using the SmarTroll probe. At a subset of these ditch locations, filtered grab samples were
327 collected and analyzed in the laboratory for Cl^- in a similar manner as for the mini and drivepoint
328 samples described above. In June 2016, the dataset was augmented for 5 ditch confluence
329 locations upstream of Spawn 1. Also in June 2016, a streambank piezometer was installed on the
330 hillslope 2.1 m lateral to the Spawn 3 cut bank to a total depth of approximately 3 m and grab
331 samples were collected after the well was cleared. A basic estimate of Darcy flux to Spawn 3
332 was made assuming a horizontal gradient, measured at 0.23 compared to stream stage on June, 5



2016 and estimated sand hydraulic conductivity of 10 m/d. Finally, for comparison to Quashnet River data the characteristic regional groundwater chemical signature of the upgradient groundwater aquifer was derived from Frimpter and Gay (1979) and Leblanc (1984) for wells outside of known contaminant influence.

Results

Only 3 small alcoves along the 2-km reach were observed to be consistently used for spawning by brook trout, all of which were associated with meander bend cut banks. Heat tracing, geophysical, and chemical methods indicate these spawning zones coincide with localized, oxic groundwater discharge.

Brook trout spatial behavior

Out of the dozens of focused seepage zones found along the Quashnet River in this and previous work (e.g. Figure 1b) brook trout appear to consistently utilize only three zones for repeat spawning activity. These locations coincide with steep cut banks where the river channel approaches the sand and gravel valley wall (Figure 2b,c). Specifically, trout were found to occupy small “scalloped” alcove bank features (Figure 3a) that may be formed by groundwater sapping and subsequent slumping of sandy bank materials. In winter 2016, fresh slumping and direct seepage from the newly exposed sand wall was observed at Spawn 3 (Figure 3c); a larger slump event had filled approximately 1/3 of the scalloped alcove at Spawn 2 by June 2016. Brook trout were observed clustered along the inner bank area at the Spawn 1 location in fall 2015 (Figure 3d), and this spawning behavior was captured using underwater video (Supplemental Video S1).

Dropout PIT tags have been located repeatedly in each of the 3 preferential spawn zones.



355 Seven dropout PIT tags were located in the Spawn 3 zone in March 2017, by far the most
356 dropped tags found in any one location since the tracking program began in 2007. The only other
357 obvious persistent scalloped bank features are located at open valley seepage Locations 14/15
358 (Figure 3b), where Location 14 is near the bank and 15 is in the thalweg. Compared to the trout
359 spawning zone alcoves (e.g. Figure 3a), this strong open valley alcove was choked with
360 watercress and thick (tens of centimeters) loose deposits of organic material and spawning trout
361 have not been observed there.

362 *Fiber-optic distributed temperature sensing*

363 The FO-DTS cables deployed at the base of both stream banks through a lower reach
364 section (Figure 2c) show differing patterns of focused seepage zones indicated by persistent,
365 cooler anomalies in Figure 4 (Briggs et al., 2017b). The cable along the downstream-right bank
366 captures a large approximately 8-m-long cooler zone at Spawn 3 (Figure 4b), and this seepage
367 signature is spatially reduced but visible along the opposing bank (Figure 4a). Other thermal
368 anomalies observed along one bank show little or no signature along the other. A short section of
369 cable (approximately 2 m) was deployed out of the water and over the fish counter apparatus,
370 and data from this zone show diurnal changes in stream water temperature lag air diurnal
371 changes by several hours (Figure 4b). Air temperature dropped noticeably over the final 1.5 d of
372 deployment (day 162), and smaller cool anomalies that appeared on warm days are no longer
373 captured by the streambed FO-DTS deployment, but the Spawn 3 signature is still visible along
374 both cables.

375 *Ground Penetrating Radar*

376 The GPR data collected along the thalweg adjacent to Spawn 1 and 2 indicate a
377 contiguous thin layer of material underlies the sandy streambed that may be peat deposited over



378 deeper sands and gravels (Figure 5a)(Briggs et al., 2017b). The GPR profile through open valley
379 seepage zone Locations 14/15 and 18 shows the strongest shallow reflectors of anywhere along
380 the open valley section. These discontinuous interface structures are interpreted as layered sand,
381 gravel, interspersed with thicker peat deposits (Figure 5b). Otherwise, discontinuous reflections
382 indicative of sediment type-interfaces of variable depth are observed near downstream open
383 valley seepage zones where attenuated GPR signals indicate thick lenses of buried peat with high
384 water content (Figure 5c).

385 *Groundwater discharge characterization*

386 Diurnal signal-based K_e measurements derived from 2 1DTempProfilers inserted in
387 sandy thalweg sediments for a month in 2014 have the same geometric mean value of $0.11 \text{ m}^2 \text{d}^{-1}$,
388 and this value is used to model vertical groundwater discharge for all locations and data
389 collection periods (Briggs, 2017). Upward fluid flux modeling is particularly sensitive to
390 sediment thermal parameters (Briggs et al., 2014), so reasonable upper and lower bounds of flux
391 magnitude were estimated as ± 1 standard deviation of the sub-daily calculations of K_e
392 ($n=732$), or a K_e range of $0.10\text{-}0.13 \text{ m}^2 \text{d}^{-1}$, which is the upper end of the general range observed
393 for interface sediments (e.g. Rau et al 2012). This uncertainty in thermal parameters could be
394 expected to generally shift the estimated flux values $\pm 0.2 \text{ md}^{-1}$ when mean values range $0.5\text{-}1.0$
395 md^{-1} , and up to $\pm 0.5 \text{ md}^{-1}$ for mean values of 3 md^{-1} (e.g. Spawn 3); however, these shifts do
396 not impact the general pattern of temporal variability observed primarily at spawn zones.

397 Sub-daily groundwater discharge fluxes evaluated over similar spring/early summer time
398 periods in 2014 and 2016 show relatively stable patterns at open valley seepage zones, generally
399 $<1 \text{ md}^{-1}$ (Figure 6a,c). At Spawn 1 and 3 seepage is stronger (2 to 3.5 md^{-1}) and more variable
400 than at open valley zones, with some apparent relation to variations in the stream water stage



401 evaluated at the USGS gage (Figure 2a). The Darcy-based horizontal seepage estimate through
402 the Spawn 3 bank, made using the bank piezometer, is 2.3 m d^{-1} , which is similar to the
403 temperature-based seepage rates at the Spawn 3 interface (Figure 6c), and indicates lateral
404 discharge through the cut bank wall from a more localized groundwater flowpath (Figure 1a).
405 The Spawn 2 zone shows a reduced and more stable discharge rate during summer 2016, and is
406 likely impacted by a large bank slump into this zone that occurred during the winter of 2016,
407 partially filling the alcove. Seepage patterns collected at Spawn 1 and 2 in late-summer 2015
408 show greater temporal stability, even though the stream stage showed substantial variation
409 (Figure 6b). Discharge rates along the inner wall of the scalloped bank spawn zones were
410 consistently higher than at bed areas located just a few meters away toward the thalweg (Figure
411 6a,b).

412 *Geochemical pore-water characterization*

413 Based on previous characterization, the regional sand and gravel aquifer generally has
414 high DO concentrations (9 - 11 mg/L), relatively dilute specific conductance (SpC, $62 \mu\text{S/cm}$),
415 and dilute chloride concentrations (Cl^- , 9.3 mg/L) at depths ranging between 12 and 20 m
416 (Savoie et al., 2012). The groundwater that discharges to the Quashnet, however, is often
417 strongly variable in all three of these parameters (Harvey et al., 2017), but SpC and Cl^- are used
418 only to indicate aquifer flowpath properties and not suitable spawn habitat as their range is well
419 within general brook trout tolerances. In June 2014, drivepoint data were primarily collected in
420 open valley seepage zones identified with FO-DTS; these locations are generally strongly
421 suboxic or anoxic at 0.3 and 0.6 m streambed depths (Table 1). The exception is Location 2 in
422 the tighter upstream valley section, which has a DO concentration of 4.6 mg/L at both depths,
423 and Spawn 3, where DO is 9.0 and 7.6 mg/L at 0.3 m and 0.6 m depths, respectively. SpC is also



424 variable, but lowest and similar to the regional signal at Location 2 and Spawn 3.

425 Drivepoint data collected at the 0.3 m depth in June 2016, primarily around spawn zones,
426 generally show high DO and relatively low SpC at the interior of Spawn Zones 1 and 3 near the
427 cut bank (Table 1). Data collected a few meters toward the thalweg from these near-bank spawn
428 locations are reduced in DO with increased SpC, in an apparent departure from the regional
429 groundwater signal. The Spawn 2 data were collected at the toe of the recent large sediment
430 slump that had partially filled the alcove, and DO data are suboxic at 0.3 m (3.9 mg/L) but more
431 oxygen enriched at 0.9 m depth (7.2 mg/L) indicating the potential for shallow streambed
432 respiration that removes oxygen from groundwater flow paths (assuming vertical flow). Spawn
433 Zones 1 and 3 are enriched and reduced in DO at the 0.9 m depth, respectively. In contrast to the
434 spawn zones, major open valley seepage Locations 14 (near scalloped bank, Figure 3b) and 15
435 (adjacent thalweg) are nearly anoxic at all depths with SpC similar to the 2014 stream water
436 profile grab samples ($n=8$, $101.4 \pm 1.7 \mu\text{S/cm}$); little difference was observed between near-
437 bank and thalweg positions.

438 The drainage-ditch grab samples generally show Cl^- concentrations that are lower than
439 the average 2014 thalweg grab samples ($n=10$, $19 \pm 0.4 \text{ mg/L}$), though the 2 most upstream
440 ditches are similar to stream water, and 2 open valley ditches are appreciably higher in Cl^-
441 (Figure 7a). Spawn Zones 1, 2, and 3 approximate the lowest Cl^- concentrations observed in
442 drainage ditches, and Spawn 3 has a similar concentration to the adjacent 2016 streambank
443 piezometer in both the 2014 and 2016 data. An analogous pattern is shown in the more
444 widespread SpC data, with many drainage ditches and all spawn zones having concentrations
445 around $60 \mu\text{S/cm}$, but several ditches cluster around the stream water average or higher,
446 particularly in the open valley area. Concentrations of DO at the drainage ditch confluences were



447 highly variable, showing no pattern with channel distance, ranging 3.1-8.4 mg/L in June 2014.

448 The shallow, discrete interval pore-water samples collected with the minipoint system
449 show that streambed SpC is appreciably lower than stream water, even at the 0.02 m depth, at all
450 near-bank spawn zones (Figure 8a). Conversely, the shallow thalweg sediments at Spawn 1 and
451 open valley seepage Location 14/15 approximate the stream water value for SpC. DO is high and
452 stable along the shallow profiles (to 0.14 m) at the interior of Spawn Zones 1 and 3, suboxic at
453 the Spawn 1 thalweg and Spawn 2 zones, and essentially anoxic at Location 14 along the entire
454 profile. Thalweg seepage Location 15 shows moderate oxygen enrichment at 0.02 m (4.6 mg/L),
455 which may result from hyporheic mixing at the 0.04-0.14 m depths that are nearly anoxic.

456 Underwater video collected here in the fall of 2015 indicates Quashnet River brook trout
457 clustered tightly around an approximate 1-m² bed area in Spawn 1 (Figure 3d, Video S1),
458 directly at the base of the sandy cut bank. During the June 2016 collection of pore-water data,
459 drivepoints were installed precisely in this area. Chemical analysis of 0.3 m depth pore water
460 shows a strong gradient from the near-bank Spawn 1 zone to the outer alcove area, with specific
461 conductance rising dramatically (70.6 to 143.9 $\mu\text{S}/\text{cm}$) and DO falling (7.28 to 4.41 mg/L)
462 (Table 1). Spawn 3 shows a similar pattern (60.4 to 82.1 $\mu\text{S}/\text{cm}$ SpC; 9.11 to 1.76 mg/L DO),
463 and Spawn 2, although complicated by the large slump during the previous winter, shows an
464 increase in SpC from 70.6 to 139.3 $\mu\text{S}/\text{cm}$ from the inner to outer alcove. Conversely, pore water
465 collected at 0.3, 0.6, and 0.9 m depths in the open valley seepage alcove at Location 14/15
466 (pictured in Figure 3b) are virtually anoxic with elevated SpC compared to inner spawn zones,
467 and little gradient from bank to thalweg. Fine-scale shallow streambed minipoint data mirror
468 these deeper samples (Figure 8).



469 Discussion

470 Heat tracing reconnaissance technology, such as FO-DTS and TIR, offer an efficient
471 means to spatially characterize a subset of focused groundwater discharge points at the reach to
472 watershed scale (e.g. Figure 1b, Figure 4). Using the groundwater-fed Quashnet River as an
473 example, Rosenberry et al. (2016) showed that cold streambed interface anomalies in summer
474 indeed corresponded to discrete zones of particularly high discharge through streambed
475 sediments. This spatial characterization alone is typically not sufficient to fully understand the
476 physical and chemical drivers of critical cold-water habitat, but it can greatly focus investigation
477 of the points of higher-weighted influence on surface water. Compared to more random
478 streambed field parameter surveys or larger spatial scale evaluations of net groundwater
479 discharge made with differential gaging, comprehensive spatial mapping of groundwater
480 discharges is a great advance in the context of understanding point-scale habitat. Here we have
481 capitalized on previous FO-DTS data collection (Figure 1b) to locate dozens of seepage zones
482 along a 2-km reach that could be assessed for temporal fluid flux dynamics and chemical
483 characteristics using subsurface data collection. However, in fast flowing streams even a few
484 meters wide, cable placement on the streambed will likely impact which specific seepage zones
485 are captured with FO-DTS, as shown here by applying cables along opposite banks through the
486 Spawn 3 area (Figure 4). The largest seepage zones may have a spatial footprint that
487 encompasses the streambed area from bank to bank (e.g., the Spawn 3 cold anomaly), but a
488 subset of more discrete seepage zones are bound to be missed with a single linear cable
489 deployment.

490 In a study of the regional Cape Cod aquifer condition, Frimpter and Gay (1979) state that
491 groundwater is typically near DO saturation, except downgradient of peat or river bottom



492 sediments, where consumption of DO allows the mobilization of natural iron and manganese.
493 Visible observations along the open valley section, in addition to streambed sediment coring
494 (Briggs et al. 2014), revealed widespread coating of shallow streambed sediment grains with
495 metal oxides, consistent with the conceptual model of organic material influence on near-surface
496 groundwater (Figure 1a). Aquifer recharge passing through upgradient groundwater flow-
497 through kettle lakes (e.g. Stouffer *et al.* 2016) may also serve to decrease the DO content of
498 regional flowpaths that discharge vertically through the bed of the Quashnet River, although we
499 hypothesize that localized peat deposits may be the primary control on both seepage zone
500 distribution and chemistry.

501 Out of the dozens of focused seepage zones located along the lower Quashnet with heat
502 tracing, most were suboxic to anoxic (Tables 1,2). Brook trout seem to consistently prefer 3 areas
503 for fall spawning, all along meander bend cut banks into the sand and gravel valley wall. Zones
504 of locally enhanced seepage, likely controlled by subtle differences in sediment hydraulic
505 conductivity, can lead to groundwater sapping of fines, reduction in bank stability, and
506 consequent slumping of bank material into the river; this process was observed in real-time at the
507 Spawn 3 meander in February 2016 (Figure 3c). Slumping effectively forms *seepage-driven*
508 alcoves outside of the main flow along banks where bed shear stress is reduced and more suitable
509 for redd placement, along with a more favorable coarse sand and gravel substrate (Bowerman et
510 al., 2014; Hausle and Coble, 1976; Raleigh, 1982).

511 In other systems, trout have been observed to occupy microhabitat around and within
512 groundwater discharge zones, even segregating by fish size and desirable temperature range
513 (e.g., Figure 2.4.1.2 in Torgersen et al. 2012). Here real-time observation and visual imagery
514 show trout clustering tightly against the bank in Spawn 3 (Figure 3d, Video S1), where pore



515 water was found to be more oxygen rich and lower in SpC. Month-long time series of bed
516 temperature-derived fluid flux show that the vertical groundwater discharge rate is reduced
517 considerably from inner to outer alcove zones, indicating a strong reduction in hydraulic gradient
518 and/or decrease in effective streambed hydraulic conductivity. The evidence of higher near-bank
519 vertical groundwater flux rates and DO, combined with lower SpC, indicates limited interaction
520 between shallow groundwater flowpaths and peat against the meander bend cut banks, resulting
521 in groundwater discharge zones most preferred by brook trout for spawning. The remote sensing
522 of streambed material with GPR indicates a relatively thin layer of streambed peat in the Spawn
523 1 and 2 thalweg area compared to open valley seepage zones (Figures 1 and 5). Therefore, it
524 appears that even short travel distances through organic deposits toward the center channel at
525 Spawn 1 and 2 may be sufficient to increase total dissolved solids and deplete DO, as observed
526 in other systems (e.g. Levy et al., 2016), and render upwelling zones undesirable for redd
527 construction. This characterization is consistent with previous GPR data collected several
528 kilometers upstream in a broad valley area in a study to assess possible naturalized channel form
529 restoration (personal communication Maggie Payne, John Cody, Melissa Kenefick, Natural
530 Resources Conservation Service, November 30, 2015). Their assessment found peat deposits >5
531 m thick in the central area of the valley, pinching out against the sands and gravels of the valley
532 walls. Cored peat sections were indicative of a buried cedar swamp, which is typical of similar
533 glacial depressions in the area (Hare et al., 2017).

534 Only where seepage was observed to emanate directly from the valley wall sands and
535 gravels, such as the newly exposed slump in Figure 3C, may groundwater discharge reliably
536 support overwinter trout egg development. These features are apparently similar to the numerous
537 cold-water alcove patches observed by Ebersole et al. (2003). In that study of preferential



538 salmonid habitat, alcoves were often located where streams converged on valley walls and were
539 the most abundant type of discrete cold-water habitat type identified. Conversely, valley wall
540 alcoves were the least-common type of seep morphology observed along the Quashnet River. It
541 is likely that the artificial reduction in channel sinuosity along the Quashnet River through
542 farming practices has reduced possible higher-quality spawning locations by focusing river flow
543 away from the valley walls and oxic groundwater discharge. Other bank alcove features with
544 strong groundwater discharge found along the open valley section (Figure 3b) were highly
545 influenced by organic material deposition and did not apparently support spawning habitat. Our
546 research indicates that in lowland systems with organic-rich floodplain sediments (e.g. Figure
547 1a), valley wall alcoves create favored brook trout spawning habitat via mineral soil-dominated
548 groundwater discharge flowpaths. It seems reasonable to infer that these features would also
549 create preferential thermal refugia in streams at times when main channel water exceeds fish
550 thermal tolerances.

551 The pore-water chemical data alone do not definitively show that seepage at the cut bank
552 spawn sites is derived from more localized groundwater recharge, as opposed to regional
553 groundwater that is unadulterated by buried peat lenses. However, the hydrodynamic data
554 derived from long-term vertical temperature profiling in seepage zones does offer additional
555 insight. In general, groundwater discharge rates are more variable at cut bank spawn zones than
556 in the open valley streambed zones (Figure 6a,c), and this variability may be tied to shorter-term
557 changes in local river stage and/or water table depth, impacting the hydraulic gradient. The
558 temporally consistent patterns of open valley discharge may be controlled by the regional
559 gradient where the flowpath-length term dominates, rendering the Darcy gradient relatively
560 insensitive to discharge zone changes in river stage or bank proximity. Previous active streambed



561 heating experiments have indicated open valley seepage to be vertical in nature to >0.6 m depth
562 also indicating regional discharge (Briggs et al., 2016a), compared to lateral local discharge
563 through the steep cut bank, indicated by the bank piezometer-stream stage lateral gradient at
564 Spawn 3.

565 Groundwater drainage-ditch data collected along the river corridor indicate low SpC/Cl⁻
566 conditions exist for the majority of ditches throughout the lower Quashnet River riparian areas
567 (Figure 7). The hillslope piezometer in sand and gravel at the down valley wall has a similar
568 chemical signature along with high DO. This similarity is further indication that low-SpC
569 groundwater discharges even to the lower portion of the river corridor, but is predominantly
570 modified chemically by travel through near-stream organics. The relic drainage ditches allow
571 discharging groundwater to effectively short circuit the valley floor peat deposits and remain
572 high in DO, similar to the natural valley wall cut bank alcoves. Future restoration strategies in
573 similar systems may consider capitalizing on this short circuit behavior, possibly by auguring
574 through buried streambed peat or movement of the stream channel toward the valley wall to
575 create more desirable brook trout aquatic habitat.

576 **Conclusions**

577 The three preferential spawn zones that have been identified over 10 yr+ of observation
578 in the 2-km study reach have strongly discharging groundwater with high DO concentration. The
579 zones are located exclusively in side alcoves of the channel created by bank slumps along
580 meanders where the river cuts into steep hillslopes along the glacial sands and gravel valley wall
581 (Figure 1a). In the alcoves at the base of the cut banks, hillslope groundwater with high DO
582 concentration is discharged through the streambed without appreciable loss of oxygen. Just a few



583 meters away toward the main channel, however, groundwater consistently discharges at lower
584 rates, is reduced in DO, and increased in SpC. The lowest oxygen concentrations in groundwater
585 are associated with water emerging from the streambed adjacent to wide riparian areas that flank
586 the Quashnet in the open valley section of the study reach. In the open valley zone, where the
587 stream is not near the valley walls, proximity to the stream bank does not seem to control
588 seepage chemistry, and GPR data indicated thick zones of discontinuous peat. In this and other
589 groundwater-dominated streams that are expected to serve as climate refugia for future native
590 trout populations, hyporheic exchange will be limited by strong upward hydraulic gradients, and
591 preferential spawning habitat may be primarily supported by discrete zones of oxic groundwater
592 upwelling at the meter to sub-meter scale as has been indicated by previous work (e.g. Curry et
593 al., 1995).

594 In systems where all groundwater discharge is anoxic, preferential salmonid spawning
595 zonation may be controlled by points of downwelling hyporheic water where shallow sediments
596 remain high in DO (Buffington and Tonina, 2009; Cardenas et al., 2016). However, these
597 hyporheic areas will deliver cold surface water to shallow sediments during winter, which may
598 impair overwintering brook trout eggs (French et al., 2016). Here, and in many other coastal
599 systems, groundwater temperature is expected to range approximately 10-12 °C, which is an
600 ideal range for egg development (Raleigh, 1982). Points of oxic groundwater upwelling devoid
601 of near-stream buried organics, combined with a recirculating side alcove and favorable sand and
602 gravel sediments, may provide ideal and unique groundwater seepage-enabled preferential
603 spawning habitat for native trout.

604 Stream surface or streambed interface heat tracing of groundwater discharge offers an
605 efficient means to locate discrete seepage zones, but offers only limited insight into the



606 groundwater hydraulics and biogeochemistry that impact localized trout habitat. A combined
607 heat tracing and valley-scale geomorphic assessment may be needed to locate probable
608 preferential seepage zones in other glacial systems, and guide stream ecological restoration
609 design. As digital elevation models become more refined and combined with infrared data
610 derived from Unmanned Aircraft Systems, remote identification of relatively small features such
611 as the seepage alcoves described here should be possible.

612 **Acknowledgements**

613 Comments from anonymous reviewers and U.S. Geological Survey (USGS) reviews by
614 Nathaniel Hitt and Paul Barlow are gratefully acknowledged. The U.S. Environmental Protection
615 Agency (USEPA) through its Office of Research and Development partially funded and
616 collaborated in the research described here under agreement number DW-14-92381701 to the
617 USGS. The USGS authors were supported by the following USGS entities: Office of
618 Groundwater, Water Availability and Use Science Program, National Water Quality Program,
619 and the Toxics Substances Hydrology Program. Field and laboratory assistance from Allison
620 Swartz, Jay Choi, Jenny Lewis, Yao Du, Danielle Hare, Courtney Scruggs, Rayna Mitzman,
621 David Rey, Geoff Delin, Eric White, MassWildlife Southeast District Staff, Jennifer Salas, and
622 volunteers from Trout Unlimited is greatly appreciated. The manuscript has been subjected to
623 Agency review and approved for publication. The views expressed in this article are those of the
624 authors and do not necessarily represent the views or policies of the USEPA. Any use of trade,
625 firm, or product names is for descriptive purposes only and does not imply endorsement by the
626 U.S. Government.

627



628 References

- 629 Annett, B., Gerlach, G., King, T. L. and Whiteley, A. R.: Conservation Genetics of Remnant
630 Coastal Brook Trout Populations at the Southern Limit of Their Distribution: Population
631 Structure and Effects of Stocking, *Trans. Am. Fish. Soc.*, 141(5), 1399–1410,
632 doi:10.1080/00028487.2012.694831, 2012.
- 633 Back, W., Baedeker, M. J. and Wood, W. W.: Scales in hydrogeology: a historical perspective, in
634 *Regional Water Quality*, pp. 11–128, Van Nostrand Reinhold, New York., 1993.
- 635 Baird, O. E. and Krueger, C. C.: Behavioral thermoregulation of brook and rainbow trout:
636 comparison of summer habitat use in an Adirondack River, New York, *Trans. Am. Fish. Soc.*,
637 132, 1194–1206, 2003.
- 638 Barlow, P. M. and Hess, K. M.: Simulated Hydrologic Responses of the Quashnet River Stream-
639 Auquifer System to Proposed Ground-Water Withdrawals, Cape Cod, Massachusetts, U.S. Geol.
640 *Surv. Rep.* 93-4064, 51, 1993.
- 641 Bowerman, T., Neilson, B. T. and Budy, P.: Effects of fine sediment, hyporheic flow, and
642 spawning site characteristics on survival and development of bull trout embryos, *Can. J. Fish.*
643 *Aquat. Sci.*, 71, 1059–1071, 2014.
- 644 Briggs, M. A.: Streambed temperature data for study of preferential brook trout spawning
645 habitat, Cape Cod, USA: U.S. Geological Survey data release, , doi:
646 <https://doi.org/10.5066/F7SQ8Z86>, 2017.
- 647 Briggs, M. A., Lautz, L. K., Buckley, S. F. and Lane, J. W.: Practical limitations on the use of
648 diurnal temperature signals to quantify groundwater upwelling, *J. Hydrol.*, 519, 1739–1751,
649 doi:10.1016/j.jhydrol.2014.09.030, 2014.
- 650 Briggs, M. A., Buckley, S. F., Bagtzoglou, A., Werkema, D. and Lane, J. W.: Actively heated
651 high-resolution fiber-optic-distributed temperature sensing to quantify streambed flow dynamics
652 in zones of strong groundwater upwelling, *Water Resour. Res.*, 52, 5179–5194,
653 doi:10.1002/2015WR018219.Received, 2016a.
- 654 Briggs, M. A., Hare, D. K., Boutt, D. F., Davenport, G. and Lane, J. W.: Thermal infrared video
655 details multiscale groundwater discharge to surface-water through macropores and peat pipes,
656 *Hydrol. Process. HPEye*, 30(14), 2510–2511, doi:10.1002/hyp.10722, 2016b.
- 657 Briggs, M. A., Lane, J. W., Snyder, C. D., White, E. A., Johnson, Z. C., Nelms, D. L. and Hitt,
658 N. P.: Shallow bedrock controls on headwater climate refugia, *Limnologica*, 1216–1225,
659 doi:10.1002/2013GL058951.Received, 2017a.
- 660 Briggs, M. A., White, E. A. and Lane, J. W.: Surface geophysical data for study of preferential
661 brook trout spawning habitat, Cape Cod, USA: U.S. Geological Survey data release, ,
662 doi:<https://doi.org/10.5066/F7PN93QF>, 2017b.
- 663 Buffington, J. M. and Tonina, D.: A three-dimensional model for analyzing the effects of salmon
664 redds on hyporheic exchange and egg pocket habitat A three-dimensional model for analyzing



- 665 the effects of salmon redds on hyporheic exchange and egg pocket habitat, *Can. J. Fish. Aquat.*
666 *Sci.*, 66, 2157–2173, doi:10.1139/F09-146, 2009.
- 667 Burns, E. R., Zhu, Y., Zhan, H., Manga, M., Williams, C. F., Ingebritsen, S. E. and Dunham, J.:
668 Thermal effect of climate change on groundwater-fed ecosystems, *Water Resour. Res.*, 2017.
- 669 Cardenas, M. B. and Wilson, J. L.: The influence of ambient groundwater discharge on exchange
670 zones induced by current-bedform interactions, *J. Hydrol.*, 331(1-2), 103–109, doi:Cited By
671 (since 1996) 36 Export Date 4 April 2012, 2006.
- 672 Cardenas, M. B., Ford, A. E., Kaufman, M. H., Kessler, A. J. and Cook, P. L. M.: Hyporheic
673 flow and dissolved oxygen distribution in fish nests: the effects of open channel velocity,
674 permeability patterns, and groundwater upwelling, *J. Geophys. Res. Biogeosciences*, 121, 3113–
675 3130, doi:10.1002/2016JG003381, 2016.
- 676 Comas, X., Slater, L. and Reeve, A. S.: Pool patterning in a northern peatland: Geophysical
677 evidence for the role of postglacial landforms, *J. Hydrol.*, 399(3-4), 173–184,
678 doi:10.1016/j.jhydrol.2010.12.031, 2011.
- 679 Crisp: A desk study of the relationship between temperature and hatching time for the eggs of
680 five species of salmonid species, *Freshw. Biol.*, 11(4), 361–368, doi:10.1111/j.1365-
681 2427.1981.tb01267.x, 1981.
- 682 Cunjak, R. A. and Power, G.: Seasonal changes in the physiology of brook trout, *Salvelinus*
683 *fontinalis* (Mitchill), in a sub-Arctic river system, *J. Fish Biol.*, 29, 279–288, 1986.
- 684 Curry, R., Noakes, D. L. G. and Morgan, G. E.: Groundwater and the incubation and emergence
685 of brook trout (*Salvelinus fontinalis*), *Can. J. Fish. Aquat. Sci.*, 52, 1741–1749, 1995.
- 686 Dugdale, S. J., Bergeron, N. E. and St-Hilaire, A.: Spatial distribution of thermal refuges
687 analysed in relation to riverscape hydromorphology using airborne thermal infrared imagery,
688 *Remote Sens. Environ.*, 160, 43–55, doi:10.1016/j.rse.2014.12.021, 2015.
- 689 Ebersole, J. L., Liss, W. J. and Frissell, C. A.: Cold water patches in warm streams:
690 physicochemical characteristics and the influence of shading, *J. Am. Water Resour. Assoc.*,
691 59860, 355–368, 2003.
- 692 French, W. E., Vondracek, B., Ferrington, L. C., Finlay, J. C. and Dieterman, D. J.: Brown trout
693 (*Salmo trutta*) growth and condition along a winter thermal gradient in temperate streams, *Can. J.*
694 *Fish. Aquat. Sci.*, 9(June), 1–9, doi:10.1139/cjfas-2016-0005, 2016.
- 695 Frimpter, M. H. and Gay, F. B.: Chemical quality of ground water on Cape Cod, Massachusetts,
696 *Water-Resources Investig. Rep.* 79-65, 1979.
- 697 Geist, D. R., Hanrahan, T. P., Arntzen, E. V, Mcmichael, G. A., Murray, C. J. and Chien, Y.:
698 Physicochemical Characteristics of the Hyporheic Zone Affect Redd Site Selection by Chum
699 Salmon and Fall Chinook Salmon in the Columbia River, *North Am. J. Fish. Manag.*, 22, 1077–
700 1085, 2002.
- 701 Grinsven, M. Van, Mayer, A. and Huckins, C.: Estimation of Streambed Groundwater Fluxes



- 702 Associated with Coaster Brook Trout Spawning Habitat, , 50(3), 432–441, doi:10.1111/j.1745-
703 6584.2011.00856.x, 2012.
- 704 Hare, D. K., Briggs, M. A., Rosenberry, D. O., Boutt, D. F. and Lane, J. W.: A comparison of
705 thermal infrared to fiber-optic distributed temperature sensing for evaluation of groundwater
706 discharge to surface water, *J. Hydrol.*, 530, 153–166, doi:10.1016/j.jhydrol.2015.09.059, 2015.
- 707 Hare, D. K., Boutt, D. F., Clement, W. P., Hatch, C. E., Davenport, G. and Hackman, A.:
708 Hydrogeological controls on spatial patterns of groundwater discharge in peatlands, *Hydrol.*
709 *Earth Syst. Sci. Discuss.*, doi:<https://doi.org/10.5194/hess-2017-282>, 2017.
- 710 Harvey, J. W. and Fuller, C. C.: Effect of enhanced manganese oxidation in the hyporheic zone
711 on basin-scale geochemical mass balance, , 34(4), 623–636, 1998.
- 712 Harvey, J. W., Choi, J. and Briggs, M. A.: Water chemistry data for study of preferential brook
713 trout spawning habitat, Cape Cod, USA: U.S. Geological Survey data release, , doi:
714 <https://doi.org/10.5066/F7BG2MG1>, 2017.
- 715 Hausle, D. A. and Coble, D. W.: Influence of sand in redds on survival and emergence of brook
716 trout (*Salvelinus fontinalis*), *Trans. Am. Fish. Soc.*, 105(1), 57–63, 1976.
- 717 Hitt, N. P., Snook, E. L. and Massie, D. L.: Brook trout use of thermal refugia and foraging
718 habitat influenced by brown trout, *Can. J. Fish. Aquat. Sci.*, 13(September), 1–13, 2017.
- 719 Hudy, M., Thieling, T. M., Gillespie, N. and Smith, E. P.: Distribution, status, and land use
720 characteristics of subwatersheds within the native range of brook trout in the Eastern United
721 States, *North Am. J. Fish. Manag.*, 28(4), 1069–1085, doi:3, 2008.
- 722 Irvine, D. J., Lautz, L. K., Briggs, M. A., Gordon, R. P. and McKenzie, J. M.: Experimental
723 evaluation of the applicability of phase, amplitude, and combined methods to determine water
724 flux and thermal diffusivity from temperature time series using VFLUX 2, *J. Hydrol.*, 531, 728–
725 737, 2015.
- 726 Irvine, D. J., Briggs, M. A., Cartwright, I., Scruggs, C. R. and Lautz, L. K.: Improved Vertical
727 Streambed Flux Estimation Using Multiple Diurnal Temperature Methods in Series,
728 *Groundwater*, (2012), 1–8, doi:10.1111/gwat.12436, 2016a.
- 729 Irvine, D. J., Briggs, M. A., Lautz, L. K., Gordon, R. P. and McKenzie, J. M.: Using Diurnal
730 Temperature Signals to Infer Vertical Groundwater-Surface Water Exchange, *Groundwater*,
731 doi:10.1111/gwat.12459, 2016b.
- 732 Isaak, D. J., Young, M. K., Nagel, D. E., Horan, D. L. and Groce, M. C.: The cold-water climate
733 shield: Delineating refugia for preserving salmonid fishes through the 21st century, *Glob. Chang.*
734 *Biol.*, 21(7), 2540–2553, doi:10.1111/gcb.12879, 2015.
- 735 Krause, S., Tecklenburg, C., Munz, M. and Naden, E.: Streambed nitrogen cycling beyond the
736 hyporheic zone: Flow controls on horizontal patterns and depth distribution of nitrate and
737 dissolved oxygen in the upwelling groundwater of a lowland river, *J. Geophys. Res.*
738 *Biogeosciences*, 118(1), 54–67, doi:10.1029/2012JG002122, 2013.



- 739 Kurylyk, B. L., MacQuarrie, K. T. B., Caissie, D. and McKenzie, J. M.: Shallow groundwater
740 thermal sensitivity to climate change and land cover disturbances: Derivation of analytical
741 expressions and implications for stream temperature modeling, Hydrol. Earth Syst. Sci., 19(5),
742 2469–2489, doi:10.5194/hess-19-2469-2015, 2015.
- 743 Kurylyk, B. L., Irvine, D. J., Carrey, S., Briggs, M. A., Werkema, D. and Bonham, M.: Heat as a
744 hydrologic tracer in shallow and deep heterogeneous media: analytical solution, spreadsheet tool,
745 and field applications, Hydrol. Process., 2017.
- 746 LeBlanc, D. R.: Sewage plume in a sand and gravel aquifer, Cape Cod, Massachusetts, U.S.
747 Geol. Surv. Water-Supply Pap. 2218, 28, 1984.
- 748 LeBlanc, D. R., Guswa, J. H., Frimpter, M. H. and Londquist, C. J.: Ground-water resources of
749 Cape Cod, Massachusetts: U.S. Geological Survey Investigations Atlas HA-692, 4 sheets, 1986.
- 750 Levy, Z. F., Siegel, D. I., Glaser, P. H., Samson, S. D. and Dasgupta, S. S.: Peat porewaters have
751 contrasting geochemical fingerprints for groundwater recharge and discharge due to matrix
752 diffusion in a large, northern bog-fen complex, J. Hydrol., 541, 941–951,
753 doi:10.1016/j.jhydrol.2016.08.001, 2016.
- 754 Lowry, C. S., Fratta, D. and Anderson, M. P.: Ground penetrating radar and spring formation in a
755 groundwater dominated peat wetland, J. Hydrol., 373(1-2), 68–79,
756 doi:10.1016/j.jhydrol.2009.04.023, 2009.
- 757 Luce, C. H., Tonina, D., Gariglio, F. and Applebee, R.: Solutions for the diurnally forced
758 advection-diffusion equation to estimate bulk fluid velocity and diffusivity in streambeds from
759 temperature time series, Water Resour. Res., 49(1), 488–506, doi:10.1029/2012WR012380,
760 2013.
- 761 MacCrimmon, H. R. and Campbell, S. C.: World Distribution of Brook Trout, *Salvelinus*
762 *fontinalis*, J. Fish. Res. Board Canada, 26(1699-1725), 1969.
- 763 Mathews, K. R. and Berg, N. H.: Rainbow trout responses to water temperature and dissolved
764 oxygen stress in two southern California stream pools, J. Fish Biol., 59, 50–67, 1997.
- 765 Modica, E.: Source and age of ground-water seepage to streams, USGS Fact Sheet Fact Sheet
766 063-99, (April), 1999.
- 767 Montgomery, D. R., Buffington, J. M., Peterson, N. P., SchuettHames, D. and Quinn, T. P.:
768 Stream-bed scour, egg burial depths, and the influence of salmonid spawning on bed surface
769 mobility and embryo survival, Can. J. Fish. Aquat. Sci., 53(5), 1061–1070, doi:10.1139/cjfas-53-
770 5-1061, 1996.
- 771 Mullan, J. W.: The sea run or “Salter” brook trout (*Salvelinus fontinalis*) fishery of the coastal
772 streams of Cape Cod, Massachusetts, Massachusetts Div. Fish. Game, Bull. 17, 1958.
- 773 Obruca, W. and Hauer, C.: Physical laboratory analyses of intergravel flow through brown trout
774 redds (*Salmo trutta fario*) in response to coarse sand infiltration, , doi:10.1002/esp.4009, 2016.
- 775 Petty, J. T., Hansbarger, J. L., Huntsman, B. M. and Mazik, P. M.: Transactions of the American



- 776 Fisheries Society Brook Trout Movement in Response to Temperature , Flow , and Thermal
777 Refugia within a Complex Appalachian Riverscape Brook Trout Movement in Response to
778 Temperature , Flow , and Thermal Refugia within a Compl, Trans. Am. Fish. Soc., 141(4),
779 1060–1073, doi:10.1080/00028487.2012.681102, 2012.
- 780 Raleigh, R. F.: Habitat suitability index models: Brook trout., U.S. Dept. Int., Fish Wildl. Serv.,
781 FWS/OBS-82, 1–42, 1982.
- 782 Rau, G. C., Andersen, M. S., McCallum, A. M., Roshan, H. and Acworth, R. I.: Heat as a tracer
783 to quantify water flow in near-surface sediments, Earth-Science Rev., 129, 40–58,
784 doi:10.1016/j.earscirev.2013.10.015, 2013.
- 785 Rezanezhad, F., Price, J. S., Quinton, W. L., Lennartz, B., Milojevic, T. and Cappellen, P. Van:
786 Structure of peat soils and implications for water storage , fl ow and solute transport : A review
787 update for geochemists, Chem. Geol., 429, 75–84, doi:10.1016/j.chemgeo.2016.03.010, 2016.
- 788 Rosenberry, D. O., Briggs, M. A., Delin, G. and Hare, D. K.: Combined use of thermal methods
789 and seepage meters to efficiently locate, quantify, and monitor focused groundwater discharge to
790 a sand-bed stream, Water Resour. Res., 52, 4486–4503, doi:10.1002/2016WR018808.Received,
791 2016.
- 792 Seitzinger, S., Harrison, J. a, Böhlke, J. K., Bouwman, a F., Lowrance, R., Peterson, B., Tobias,
793 C. and Van Dreht, G.: Denitrification across landscapes and waterscapes: a synthesis., Ecol.
794 Appl., 16(6), 2064–90 [online] Available from: <http://www.ncbi.nlm.nih.gov/pubmed/17205890>,
795 2006.
- 796 Snook, E. L., Letcher, B. H., Dubreuil, T. L., Zydlewski, J., Donnell, M. J. O., Whiteley, A. R.,
797 Hurley, S. T. and Danylchuk, A. J.: Movement patterns of Brook Trout in a restored coastal
798 stream system in southern Massachusetts, Ecol. Freshw. Fish, 26, 360–375,
799 doi:10.1111/eff.12216, 2016.
- 800 Stoliker, D. L., Repert, D. A., Smith, R. L., Song, B., Leblanc, D. R., Mccobb, T. D., Conaway,
801 C. H., Hyun, S. P., Koh, D., Moon, H. S. and Kent, D. B.: Hydrologic Controls on Nitrogen
802 Cycling Processes and Functional Gene Abundance in Sediments of a Groundwater Flow-
803 Through Lake, Environ. Sci. Technol., 50, 3649–3657, doi:10.1021/acs.est.5b06155, 2016.
- 804 Wehrly, K., Wang, L. and Mitro, M.: Field-based estimates of thermal tolerance limits for trout:
805 incorporating exposure time and temperature fluctuation, Trans. Am. Fish. Soc., 136, 365–374,
806 2007.
- 807 Winter, T. C., Harvey, J. W., Franke, O. L. and Alley, W. M.: Ground water and surface water; a
808 single resource, Gr. Water U . S . Geol. Surv. Circ. 1139, 79, 1998.

809

810



811 Tables

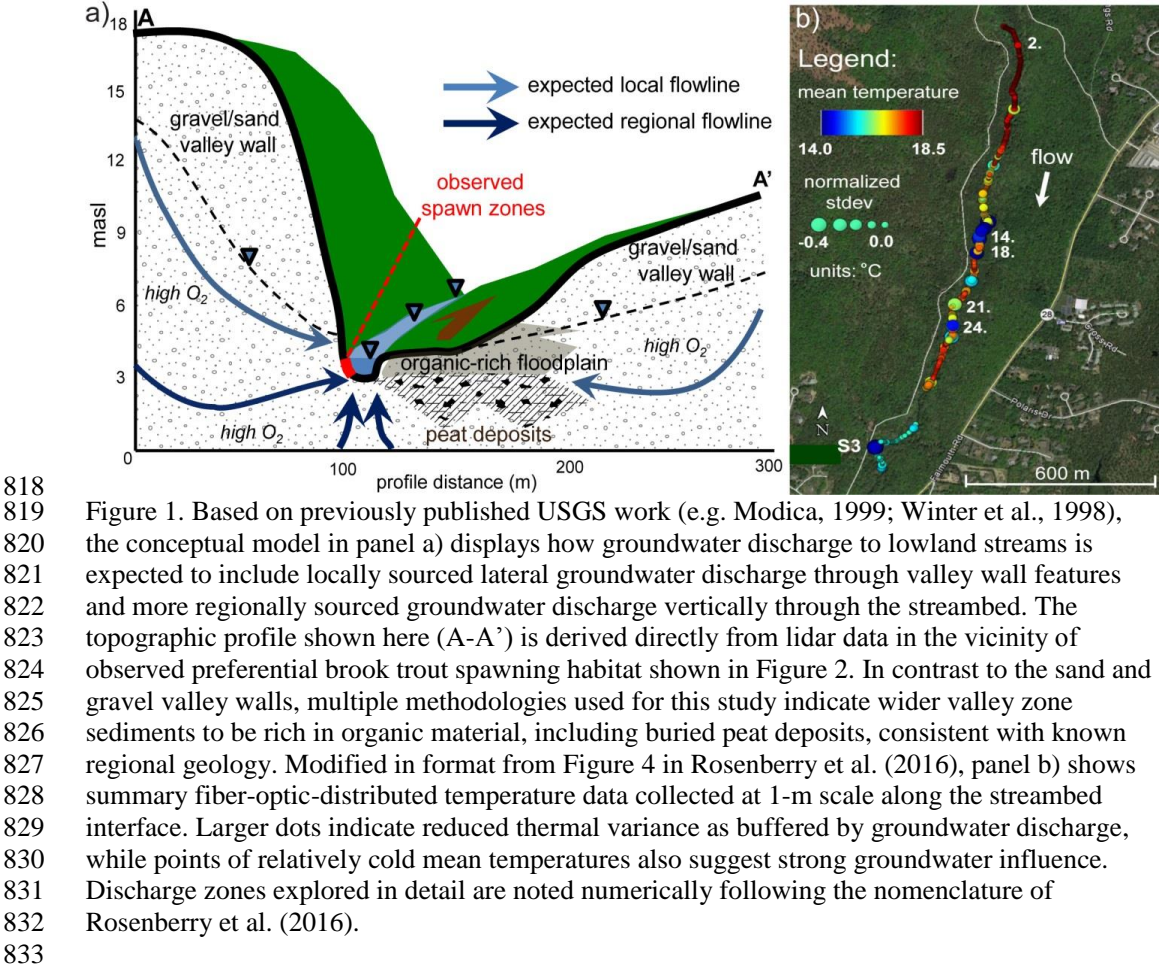
812 Table 1. 2014 and 2016 drivepoint pore-water chemistry data collected in major streambed
 813 groundwater seepage zones located with fiber-optic heat tracing, and in zones of observed repeat
 814 trout spawning directly along the bank (“in”) and farther toward the stream thalweg (“out”).

<i>June 2014 Location</i>	<i>0.3 m depth</i>		<i>0.6 m depth</i>	
	DO mg/L	SpC μS/cm	DO mg/L	SpC μS/cm
Location 2	4.6	53.8	4.6	61.3
Location 4	1.4	97.7	3.4	65.1
Location 15	0.1	78.8	0.0	82.5
Location 18	0.2	100.0	0.2	89.8
Location 21	0.0	77.7	0.0	79.0
Location 24	0.1	69.1	0.0	64.3
Location 27	1.4	75.0	0.5	79.4
Spawn 3 in	9.0	56.4	7.6	60.9
<i>June 2016 Location</i>	<i>0.3 m depth</i>		<i>0.9 m depth</i>	
Spawn 1 in	7.28	70.6	9.76	55.9
Spawn 1 out	4.41	143.9	5.68	143.2
Spawn 2 in	3.89	70.8	7.17	57.6
Spawn 2 out	5.25	139.3	n/a	n/a
Spawn 3 in	9.11	60.4	4.91	71.9
Spawn 3 out	1.76	82.1	2.68	79.9
Location 15 in	0.16	105.5	0.39	104.0
Location 15 out	0.31	99.1	0.18	96.4

815
 816



Figure List



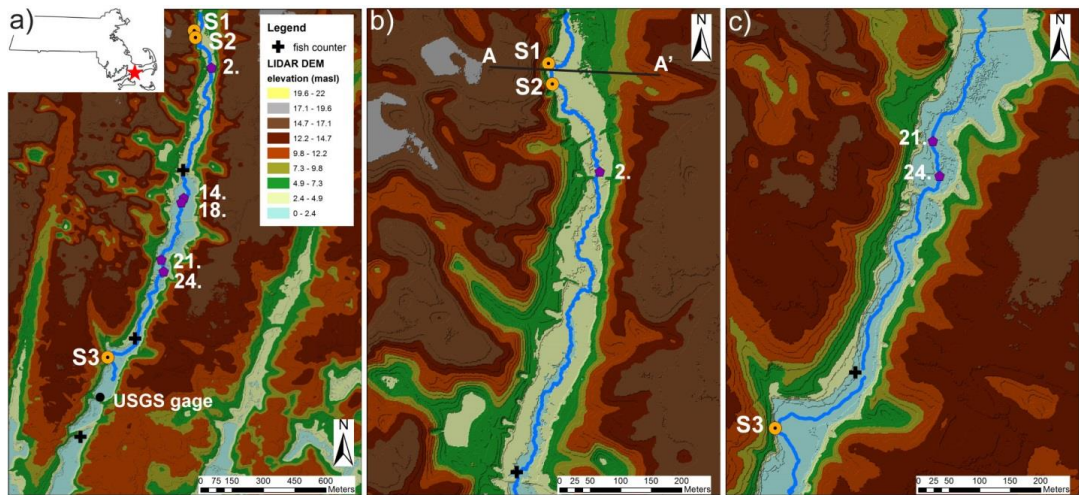


Figure 2. Lidar elevation data show the linear valley terrain of: a) The lower Quashnet River reach with Spawn (S1, S2, S3) locations (orange circles) and open valley seepage zones (purple circles) identified. Panel b) shows the tighter upper valley zone where Spawn 1 and 2 are located at the base of a steep cut bank and the topographic transect of Figure 1 is noted. Panel c) displays the lower open valley reach where Spawn 3 is located along a cut bank.



Figure 3. Images collected in February 2016 a) the cut bank alcove at Spawn 1, b) open valley seepage Location 14/15, and c) fresh cut bank slumping and visible seepage Spawn 3. Panel d) is an image from the underwater video collected in fall 2015 of spawning trout in the alcove pictured in panel a), showing several fish clustered around the sandy zone directly at the base of the cut bank.

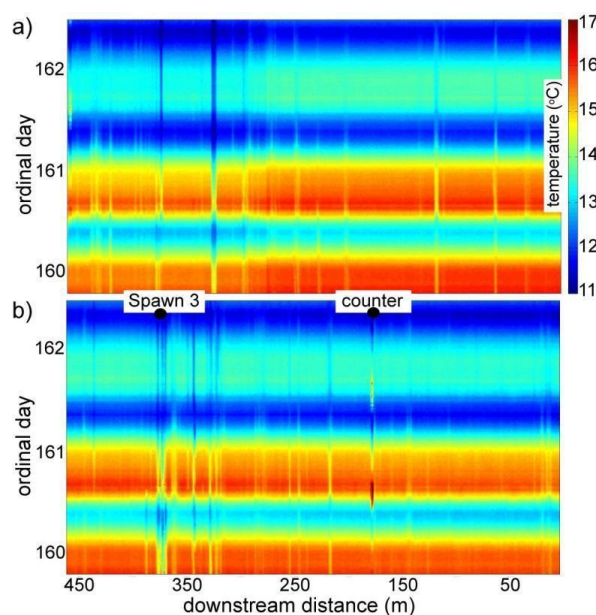


Figure 4. Fiber-optic-distributed temperature data collected starting at an arbitrary stream point along a) the downstream left bank and b) the downstream right bank through the Spawn 3 meander bend area (see Figure 2c for location). The vertical bands of cooler (blue) colors indicate discrete groundwater discharge; some larger zones display a thermal signature on both banks while smaller discharges may be bank-specific.

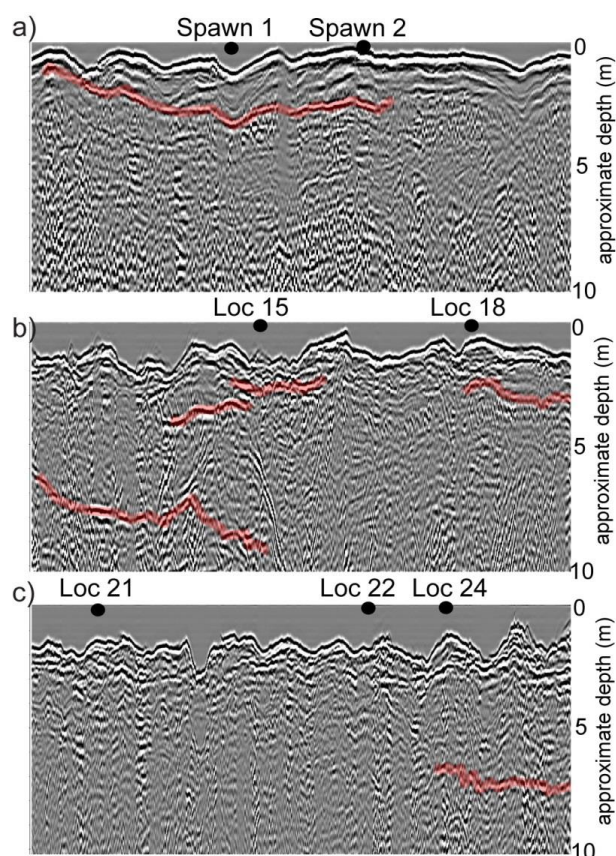


Figure 5. Quashnet River thalweg ground penetrating radar profiles were collected in the vicinity of: a) Spawn 1 and 2; b) open valley seepage Locations 15 and 18; and c) open valley seepage Locations 21, 22, and 24. Stronger apparent reflectors are highlighted in red, and likely indicate sediment layer boundaries (e.g. sand/gravel and peat).

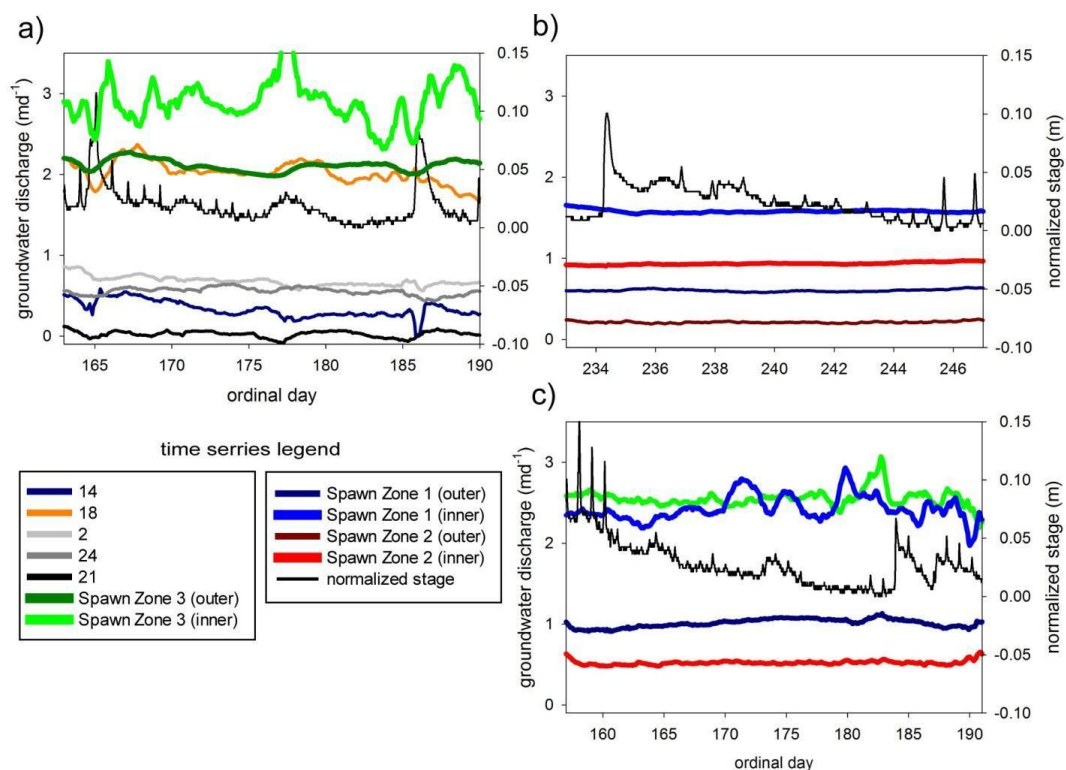


Figure 6. The Quashnet River USGS gaging station stage is compared to sub-daily time series of vertical groundwater flux rate at various strong seepage zones in a) June 2014, b) August 2015, and c) June 2016.

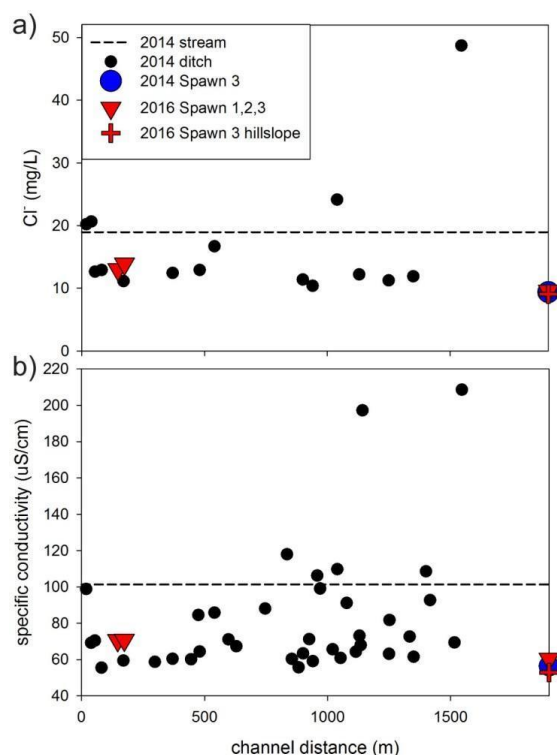


Figure 7. Drainage ditch chemistry throughout the lower Quashnet showing a) Cl^- , and b) specific conductance, collected in June 2014 just above the confluence with the main channel. Data are plotted as distance from the upper flood control structure in the narrow valley reach and compared to groundwater seepage data collected in preferential spawning locations and a hillslope piezometer.

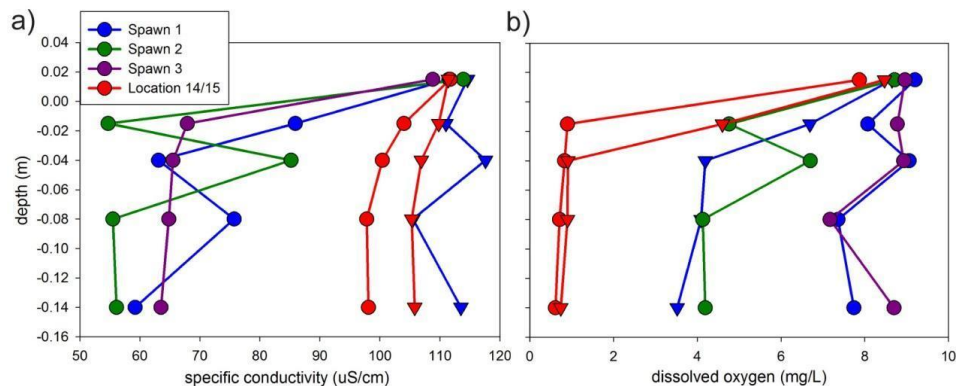


Figure 8. Minipoint pore-water chemistry data showing high spatial resolution profiles of a) specific conductance, and b) dissolved oxygen, collected in June 2016 at the major seepage alcoves. Triangle symbols indicate data collected farther toward the thalweg from the respective alcove bank, and all profiles include a local stream water sample taken just above the streambed interface.

Supplemental

Supplemental Video S1. Underwater video of brook trout spawning in the fall of 2015 (still image Figure 3d).